Bioorganic & Medicinal Chemistry Letters 22 (2012) 4599–4604

Contents lists available at SciVerse ScienceDirect

Bioorganic & Medicinal Chemistry Letters

journal homepage: www.elsevier.com/locate/bmcl

Discovery of novel benzylidene-1,3-thiazolidine-2,4-diones as potent and selective inhibitors of the PIM-1, PIM-2, and PIM-3 protein kinases

Les A. Dakin [a], Michael H. Block [a], Huawei Chen [a], Erin Code [a], James E. Dowling [a], Xiaomei Feng [a], Andrew D. Ferguson [b], Isabelle Green [c], Alexander W. Hird [a], Tina Howard [d], Erika K. Keeton [a], Michelle L. Lamb [a,*], Paul D. Lyne [a], Hannah Pollard [c], Jon Read [d], Allan J. Wu [a], Tao Zhang [a], Xiaolan Zheng [a]

[a] Oncology iMed Sciences Group, AstraZeneca R&D Boston, 35 Gatehouse Drive, Waltham, MA 02451, USA
[b] Discovery Sciences – Structure and Biophysics, AstraZeneca, 35 Gatehouse Drive, Waltham, MA 02451, USA
[c] Discovery Sciences – Reagents and Assay Development, AstraZeneca, Alderley Park, Cheshire SK10 4TG, UK
[d] Discovery Sciences – Structure and Biophysics, AstraZeneca, Alderley Park, Cheshire SK10 4TG, UK

ARTICLE INFO

Article history:
Received 26 March 2012
Revised 18 May 2012
Accepted 29 May 2012
Available online 6 June 2012

Keywords:
PIM kinases
Hit-to-lead
Small molecule inhibitor
Thiazolidine-2,4-dione
X-ray crystallography
Cancer

ABSTRACT

Novel substituted benzylidene-1,3-thiazolidine-2,4-diones (TZDs) have been identified as potent and highly selective inhibitors of the PIM kinases. The synthesis and SAR of these compounds are described, along with X-ray crystallographic, anti-proliferative, and selectivity data.

The PIM kinases (PIM-1, 2, and 3) (proviral integration site for moloney murine leukemia virus) are a family of three serine/threonine kinases which constitute a small family of enzymes with a high degree of sequence and structural homology. They were identified as oncogenes[1] and found to synergize with c-Myc for lymphomagenesis in transgenic mouse models.[2] The PIM kinases are primarily regulated by growth factor and cytokine signaling downstream of PTK/STAT activation.[3] In contrast to the majority of other kinases, PIM kinases are constitutively active enzymes whose activity is largely regulated by their post-transcriptional and post-translational (protein stability) levels. These kinases are also unusual in the structure of their kinase domains, where the hinge region of the ATP-binding pocket contains a proline residue not found in other kinases. This results in a molecular recognition motif that is unique among the kinase family.[4] Additionally, the PIM kinases have pleiotropic roles, but the primary functions of these kinases are in promoting proliferation, through direct phosphorylation of cell cycle regulators (Cdc25A, Cdc25C, p21 and p27), and cell survival, at least in part through phosphorylation and inactivation of the pro-apoptotic BAD protein.[5] Gene knockout studies have demonstrated that mice deficient in all three PIM kinases are small but viable and fertile.[6] PIM kinases are also overexpressed in a number of human tumors. PIM-1 and PIM-2 proteins are commonly found in haematological malignancies and prostate tumors, while elevated PIM-3 expression is observed with several different solid tumors. Deregulated PIM kinase expression is linked to genetic aberrations such as FLT3-ITD in AML[7] and BCR-ABL in CML.[8] In addition, aberrant somatic hypermutation of PIM-1 is characteristic of diffuse large B-cell lymphoma, as well as follicular lymphoma, Hodgkin's lymphoma and MALT (mucosa-associated lymphoid tissue).[9] PIM proteins have been found to interact with the transcription factor Myc in promoting oncogenesis in prostate cancer,[10] as well as lymphoma,[2] and high PIM-1 expression levels have been correlated to poor radiation therapy response in squamocellular head and neck cancer.[11] These and other accumulating evidence support the importance of the PIM kinases in tumor initiation, progression, and maintenance.

On embarking on the design of potent PIM inhibitors, a key consideration was the proline in the hinge region of the ATP binding site which is not found in other kinases. This cyclic residue alone sequesters the backbone nitrogen required to donate a hydrogen

* Corresponding author.
E-mail address: Michelle.Lamb@astrazeneca.com (M.L. Lamb).

0960-894X/$ - see front matter © 2012 Published by Elsevier Ltd.
http://dx.doi.org/10.1016/j.bmcl.2012.05.098

bond to the adenine ring of ATP, and thus, conventional ATP-competitive kinase inhibitors are not optimized for this site. Although this feature presented a challenge, we felt this also afforded an opportunity to develop inhibitors selective against other kinases. Our goal was to identify inhibitors capable of pan-PIM inhibition, since the biological roles of the isozymes could be redundant in some circumstances, and the active site homology between family members appeared to support this strategy (PIM-1 and PIM-2 are 85% identical; PIM-1 and PIM-3, 93%). A broad high-throughput screen against PIM-2 to identify ATP competitive compounds was undertaken and (5*Z*)-5-(3-ethoxy-4-hydroxybenzylidene)-1,3-thiazolidine-2,4-dione (**1**), which is commercially available from the ChemBridge Corporation, was identified as a 0.16 μM inhibitor of the PIM-2 kinase (Fig. 1). Interestingly, other thiazolidine-2,4-diones (TZDs) have independently been reported in the literature as PI3Kγ, PIM, and CDK2 kinase inhibitors.[12–14]

We chose to pursue **1** for further studies since it was highly ligand efficient[15] (by pIC_{50}/number of heavy atoms method, LE = 0.38) and there were opportunities to expand the SAR around the aryl ring. We were interested to determine whether or not we could remove the phenol from the series, as phenols often give poor pharmacokinetic and drug-like properties. To do this we first synthesized a variety of substituted benzylidene-1,3-thiazolodine-2,4-diones (TZDs) via a Knoevenagel condensation[16] with 2,4-thiazolidinedione (**2**) and a variety of substituted benzaldehydes (**3**) (Scheme 1, Eq. 1).[17]

The compounds initially synthesized, examples **6** and **7** (Table 1), were still modestly potent which suggested to us that the TZD was the critical binding element for this scaffold. This moiety was expected to be quite acidic, and the pK_a of the unsubstituted analog **7** was found to be 6.14. Structure-based design, utilizing SAR from additional HTS hits, led us to next investigate effects of amine substitution ortho to the TZD moiety on the aromatic core (position R^1). The required benzaldehyde substrates were readily prepared via a nucleophilic aromatic substitution with various amine bases in the presence of K_2CO_3 in heated DMSO or refluxing acetonitrile (Scheme 1, Eq. 2). Incorporation of the basic amine, *N,N*-dimethylpyrrolidin-3-amine, at the R^1 position of the scaffold afforded compound **8**, which had potency against all three isoforms of the enzyme comparable to compound **1** and was devoid of the phenol. The Boc protected analog **9** was significantly less potent than its deprotected counterpart (**11**), and notably, all other synthesized analogs that did not incorporate a basic amine on the molecule showed significantly diminished activity (not shown). Of all the amines explored, cyclic primary amines, such as the (3*S*)-pyrrolidin-3-amine (**11**) and (3*R*)-piperidin-3-amine (**15**) examples, were most effective. Interestingly, these chiral examples showed only a slight potency advantage over their corresponding enantiomers. It was also discovered that incorporation of chlorine adjacent the (3*S*)-pyrrolidine-3-amine at position R^2 (**12**) conferred a 10-fold increase in enzyme potency over its matched pair (**11**), with inhibitory potencies of this example approaching the limit of detection of our K_m [ATP] enzyme assays.[18] Substitution instead at the R^3 position of the ring (**13**) had a less pronounced effect on enzyme potency.

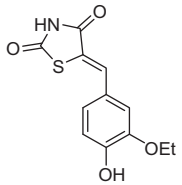

1, PIM-2 IC_{50}: 0.16 μM

Figure 1. The TZD PIM-2 HTS hit.

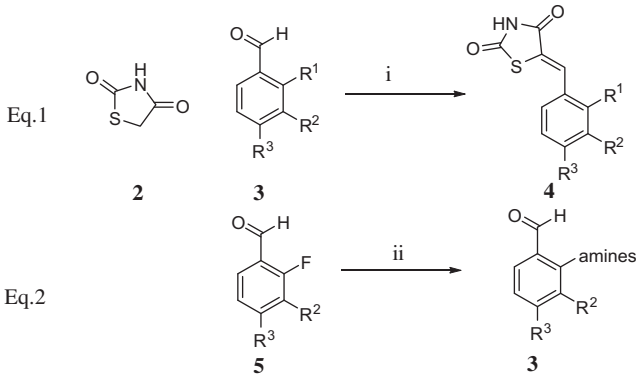

Scheme 1. Reagents and conditions: (i) piperidine (5 mol %), ethanol, reflux, (50–90%), *Z*/*E* (>98:2); (ii) amine, K_2CO_3, MeCN (reflux) or DMSO (80 °C) (40–88%).

Given the observed importance of both the acidic TZD and basic amine to potency, the binding of these ligands was expected to involve an interaction of the TZD moiety with the conserved lysine residue (Lys 67) and placement of the amine into the carboxylate-rich ribose binding pocket. Indeed, several small molecule PIM inhibitors have been disclosed to date that indicate the importance of a ligand–protein interaction with the conserved lysine.[13b,19] This binding mode would place the chlorine of **12** adjacent to hydrophobic residues within the site, near the region known as the solvent channel. We chose next to examine further the effect of hydrophobic substitution at this position of the scaffold. To develop the SAR, we maintained the optimal (3*R*)-piperidin-3-amine base and synthesized derivatives varying the size and nature of the group at the R^2 position of the scaffold. The halogenated derivatives (**22**, **23**) were synthesized according to Scheme 1 starting from commercially available benzaldehydes. The alkoxy derivatives (**24**–**27**), could readily be synthesized from commercially available 2-fluoro-3-hydroxybenzonitrile (**16**). Alkylation of the phenol with the appropriate alkyl bromide and K_2CO_3 in acetonitrile at 60 °C afforded alkylated derivatives **17** in good yield. Functional group interconversion of the nitrile to the aldehyde with Dibal-H provided the desired 2-fluoro-3-alkoxybenzaldehyde substrates (**18**) (Scheme 2, Eq. 1). The benzaldehydes **18** were then subjected to the S_NAr reaction with *tert*-butyl (3*R*)-piperidin-3-ylcarbamate to yield the desired Knoevenagel substrates. The aromatic (**28**) and heteroaromatic (**29**) derivatives were synthesized starting from 3-bromo-2-fluorobenzaldehyde (**19**). First, a S_NAr reaction with *tert*-butyl (3*R*)-piperidin-3-ylcarbamate was performed using conditions described previously. This furnished the amine substituted compound **20**, which could then be converted to the desired derivatives, **21**, via a Suzuki coupling under standard conditions (Scheme 2, Eq. 2). The resulting substituted benzaldehydes (**21**) were then converted into their corresponding final compounds via the Knoevenagel protocol illustrated in Scheme 1 followed by Boc-deprotection of the (3*R*)-piperidin-3-amine.

Continued exploration of the R^2 position of the scaffold proved an effective strategy since incorporation of hydrophobes at this position, (chlorine (**22**), bromine (**23**), alkoxy (**24**–**27**), and phenyl (**28**)), afforded inhibitors at or beyond the level of detection of our K_m [ATP] enzyme assays, < 3 nM against all PIM isoforms (Table 2). Notably, more polar heteroaromatic groups such as pyridine (**29**) were less tolerated, especially against PIM-2.

An X-ray crystal structure of **27** in PIM-1 (residues 29–313) was obtained to confirm its binding mode (Fig. 2). There is, as expected, a close interaction of the TZD with the conserved lysine (TZD N–Lys NZ 2.9 Å) and also the backbone NH of Asp 186 (TZD O–Asp N 2.9 Å,

Table 1
SAR of the aromatic core (IC_{50}, μM, [ATP] at K_m)[18]

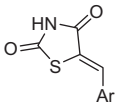

Compd	Ar	PIM-1	PIM-2	PIM-3
1	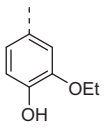	0.16	0.16	0.39
6	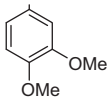	0.95	2.5	0.28
7		0.89	4.7	0.73
8	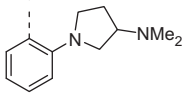	0.061	0.50	0.11
9	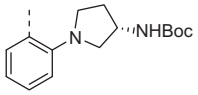	1.5	15	3.2
10	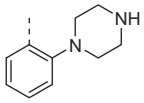	0.028	0.18	0.036
11	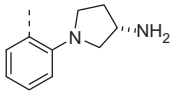	0.036	0.25	0.042
12	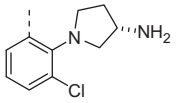	<0.006	0.025	<0.005
13	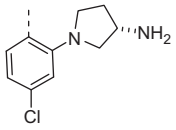	0.012	0.079	0.005
14	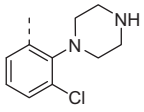	0.018	0.082	0.026
15	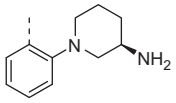	0.009	0.014	0.009

not shown). The more buried carbonyl oxygen at the 2-position of the TZD displaces a water molecule often found in other PIM-1-ligand structures, for example that interacting with a triazolopyridazine in PDB: 3BGQ.[19b] The primary amine is positioned between the receptor carboxylate of Asp 128 and the backbone oxygen of Glu 171 in the ribose pocket. Two crystallographic waters are nearby, one of which interacts with the sidechain of Glu 171. An additional water molecule is located near the 4-carbonyl of the TZD and is centered beneath the sidechain of the P-loop Phe 49 (water O–Phe ring center, 3.4 Å). The hydrophobic isopropyl group is positioned between the hydrophobic residues Val 126, Leu 44 (not

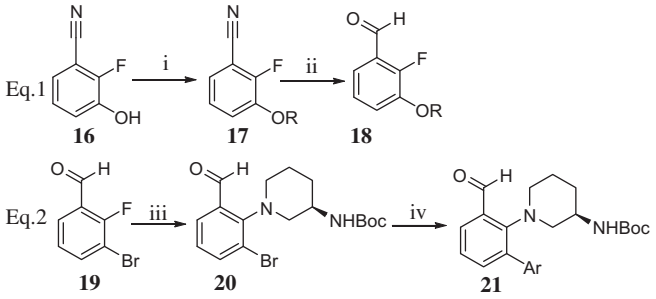

Scheme 2. Reagents and conditions: (i) alkyl bromide, K_2CO_3, MeCN, 60 °C (65–88%); (ii) Dibal-H, PhMe, 0 °C→rt (65–90%); (iii) *tert*-butyl (3*R*)-piperidin-3-ylcarbamate, K_2CO_3, MeCN, reflux (70%); (iv) $ArB(OH)_2$, $Pd(dppf)Cl_2$, Na_2CO_3, dioxane/water (5:1), reflux, (50–75%).

Table 2
Effect of substitution at the R^2 position (IC_{50}, μM, [ATP] at K_m)[18]

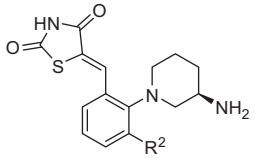

Compd	R^2	PIM-1	PIM-2	PIM-3
15	H	0.009	0.014	0.009
22	Cl	<0.003	0.005	<0.003
23	Br	<0.003	<0.003	<0.003
24	OMe	<0.003	0.005	<0.003
25	OEt	<0.003	<0.004	<0.003
26	*i*-BuO	<0.003	<0.004	<0.003
27	*i*-PrO	<0.003	<0.003	<0.003
28	Ph	<0.003	0.005	<0.003
29	4-Pyridyl	<0.003	0.019	0.004

shown), and Leu 174. For PIM-2, the residue analogous to Val 126 is an alanine, and the increased potency against this isozyme with substitutions at R^2 (compared to **15,** R^2 = H, Tables 2 and 3) can be rationalized by an increase in contact at this position. The observed binding mode for **27** is consistent with the experimental pK_a values determined for compound **28**, (5.95 for the N–H of the TZD and 9.83 for the (3*R*)-piperidin-3-amine), and differs from earlier TZD-PIM-1 binding modes that have been described in which the thiazolidine-2,4-dione is found to interact with the lysine with the carbonyl at the 4-position of the ring directed into the selectivity pocket.[13b] While this manuscript was being prepared, two additional TZD crystal structures were reported that further support the influence of the substitution pattern of the phenyl ring on the observed binding modes in PIM-1.[20]

In order to differentiate between the most potent examples (**15**, **22**–**28**) we evaluated them in enzyme assays with high substrate concentration ([ATP] = 5 mM) to better approximate intracellular concentrations. Additionally, we further profiled these inhibitors in cell proliferation, metabolic stability, aqueous solubility, and hERG activity assays (Table 3). Our inhibitors showed good antiproliferative activity in a megakaryoblastic leukemia cell line, MOLM-16, with GI_{50} values less than 100 nM.[22] All of the leading examples exhibited low in vitro rat clearances (<12.1 μL/min/mg), excellent aqueous solubilities, and low activity in the hERG ion channel assay, which predicts for cardiac QT prolongation.[23]

An early representative of the series with potency against all three isozymes (Table 2), compound **23** was tested against a panel of 441 kinases at a single concentration of 1.0 μM to assess its

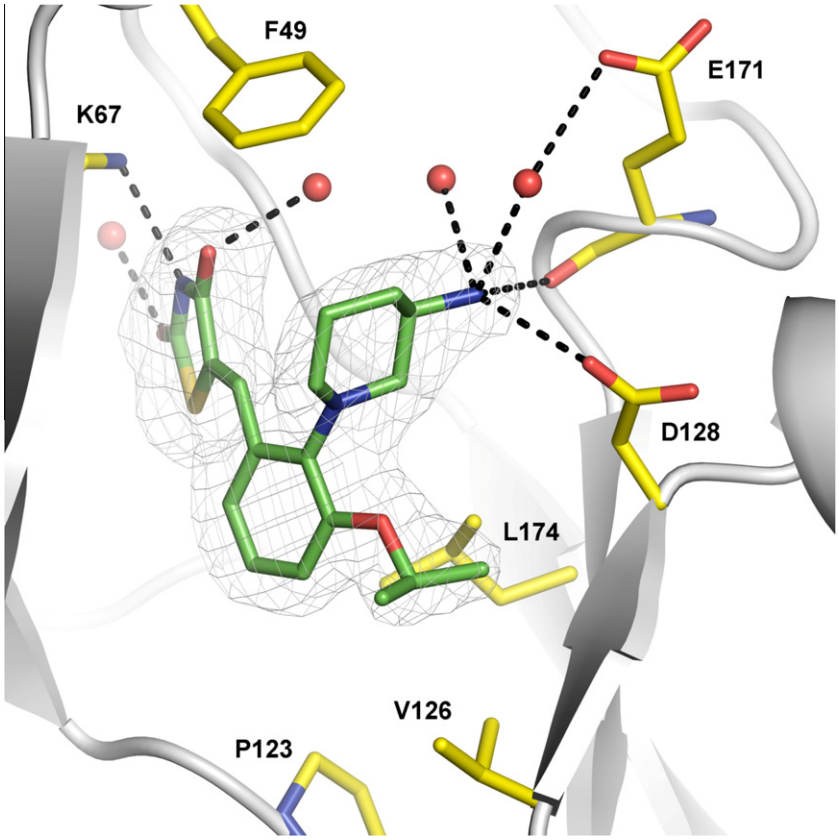

Figure 2. Human PIM-1 kinase in complex with **27** (PDB code: 4DTK). The structure is oriented with the N-terminal lobe towards the top left, the C-terminal lobe towards the bottom right and the hinge region on the bottom left. Main chain is shown as a cartoon and selected residues of the protein are depicted with yellow carbon atoms. Carbon atoms of **27** are shown in green. The electron density ($2F_o - F_c$), contoured at 1σ, is shown as a wire mesh. Polar interactions ⩽3.0 Å are shown as dotted lines. The P-loop has been removed for the purposes of clarity.[21]

Table 3
Leading examples tested in PIM-1,-2, and -3 enzyme assays at high [ATP] = 5 mM (IC_{50}, μM), MOLM-16 (GI_{50}, μM), rat microsomal stability (Cl_{int}, μL/min/mg), aqueous solubility (μM), and hERG channel inhibition (IC_{50}, μM)

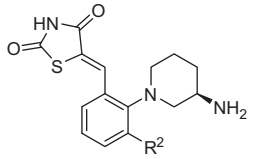

Compd	R^2	PIM-1	PIM-2	PIM-3	MOLM-16	Microsomal stability	Solubility	hERG
15	H	0.10	1.20	0.24	0.49	<4.8	782	>30
22	Cl	0.02	0.31	0.02	0.19	8.8	527	>30
23	Br	0.01	0.15	0.01	0.10	<4.8	>720	>30
24	OMe	0.02	0.32	0.01	0.21	3.9	>1000	>30
25	OEt	0.01	0.16	0.006	0.08	12.1	>1000	>30
26	*i*-BuO	0.008	0.14	<0.003	0.08	6.9	337	23
27	*i*-PrO	<0.004	0.05	<0.003	0.02	<4.8	378	>30
28	Ph	<0.003	0.15	0.009	0.02	<4.8	263	>30
29	4-Pyr	0.004	0.69	0.038	2.28	—	142	>30

selectivity profile (Fig. 3). The Ambit KINOME*scan*™ technology employs a competition binding assay that measures the ability of a compound to compete with an immobilized, active-site directed ligand.[24] The three PIM kinases were the top hits with the highest percentage of competition, and only 13 additional kinases (13/441, 2.9%) were inhibited by greater than 50%. Neither PI3Kγ nor CDK2 were inhibited at this concentration.

In summary, we have described a novel class of TZDs which are potent and selective inhibitors of the PIM family of kinases. Starting from the micromolar PIM-2 HTS hit **1**, we were able to advance the series to examples with low nanomolar activity against all three PIM isoforms. We have elucidated the binding mode, and in so doing, demonstrated the significance of the interaction between the TZD and the conserved lysine. Addition-

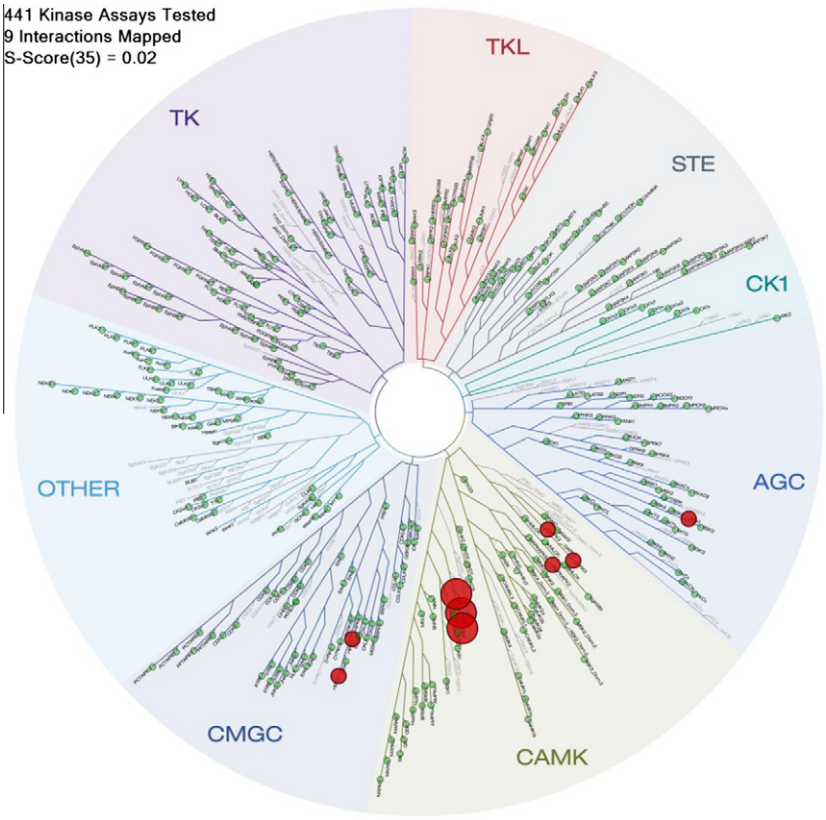

Figure 3. Example **23** tested in the Ambit kinase selectivity panel. Red circles correspond to kinases that are inhibited >65%, with size proportional to activity.[25]

ally, we have shown the beneficial effects on the potency of this series through the incorporation of basic amines into the ribose pocket and the strategic placement of hydrophobic groups. Significantly, these inhibitors have been demonstrated to have good anti-proliferative activity in the MOLM-16 cell line, high in vitro stability, limited hERG activity, and high aqueous solubilities. As such, this series of PIM inhibitors is currently under further investigation, and those findings will be reported in due course.

Supplementary data

Supplementary data associated with this article can be found, in the online version, at http://dx.doi.org/10.1016/j.bmcl.2012.05.098.

References and notes

1. Cuypers, H. T.; Selten, G.; Quint, W.; Zijlstra, M.; Maandag, E. R.; Boelens, W.; van Wezenbeek, P.; Melief, C.; Berns, A. *Cell* **1984**, *37*, 141.
2. van Lohuizen, M.; Verbeek, S.; Krimpenfort, P.; Domen, J.; Saris, C.; Radaszkiewicz, T.; Berns, A. *Cell* **1989**, *56*, 673.
3. Wang, Z.; Bhattacharya, N.; Weaver, M.; Petersen, K.; Meyer, M.; Gapter, L.; Magnuson, N. S. *J. Vet. Sci.* **2001**, *2*, 167.
4. Qian, K. C.; Wang, L.; Hickey, E. R.; Studts, J.; Barringer, K.; Peng, C.; Kronkaitis, A.; Li, J.; White, A.; Mische, S.; Farmer, B. *Biol. Chem.* **2005**, *280*, 6130.
5. Nawijn, M.; Alendar, A.; Berns, A. *Nat. Rev. Cancer* **2011**, *11*, 23.
6. Mikkers, H.; Nawijn, M.; Allen, J.; Brouwers, C.; Verhoeven, E.; Jonkers, J.; Berns, A. *Mol. Cell Biol.* **2004**, *24*, 6104.
7. Kim, K. T.; Baird, K.; Ahn, J. Y.; Meltzer, P.; Lilly, M.; Levis, M.; Small, D. *Blood* **2005**, *105*, 1759.
8. Nieborowska-Skorska, M.; Hoser, G.; Kossev, P.; Wasik, M. A.; Skorski, T. *Blood* **2002**, *99*, 4531.
9. Pasqualucci, L.; Neumeister, P.; Goossens, T.; Nanjangud, G.; Chaganti, R. S. K.; Küppers, R.; Dalla-Favera, R. *Nature* **2001**, *412*, 341.
10. Wang, J.; Kim, J.; Roh, M.; Franco, O. E.; Hayward, S. W.; Wills, M. L.; Abdulkadir, S. A. *Oncogene* **2010**, *29*, 2477.
11. Peltola, K.; Hollmen, M.; Maula, S.-M.; Rainio, E.; Ristamäki, R.; Luukkaa, M.; Sandholm, J.; Sundvall, M.; Elenius, K.; Koskinen, P. J.; Grenman, R.; Jalkanen, S. *Neoplasia* **2009**, *11*, 629.
12. Knight, S. D.; Adams, N. D.; Burgess, J. L.; Chaudhari, A. M.; Darcy, M. G.; Donatelli, C. A.; Luengo, J. I.; Newlander, K. A.; Parrish, C. A.; Ridgers, L. H.; Sarpong, M. A.; Schmidt, S. J.; Van Aller, G. S.; Carson, J. D.; Diamond, M. A.; Elkins, P. A.; Gardiner, C. M.; Garver, E.; Gilbert, S. A.; Gontarek, R. R.; Jackson, J. R.; Kershner, K. L.; Luo, L.; Raha, K.; Sherk, C. S.; Sung, C.-M.; Sutton, D.; Tummino, P. J.; Wegrzyn, R. J.; Auger, K. R.; Dhanak, D. *ACS Med. Chem. Lett.* **2010**, *1*, 39; (b) Camps, M.; Rückle, T.; Ji, H.; Ardissone, V.; Rintelen, F.; Shaw, J.; Ferrandi, C.; Chabert, C.; Gillieron, C.; Françon, B.; Martin, T.; Gretener, D.; Perrin, D.; Leroy, D.; Vitte, P.-A.; Hirsch, E.; Wymann, M. P.; Cirillo, R.; Schwarz, M. K.; Rommel, C. *Nat. Med.* **2005**, *11*, 936.
13. (a) Xia, Z.; Knaak, C.; Ma, J.; Beharry, Z. M.; McInnes, C.; Wang, W.; Kraft, A. S.; Smith, C. D. *J. Med. Chem.* **2009**, *52*, 74; (b) Miduturu, C. V.; Deng, X.; Kwiatkowski, N.; Yang, W.; Brault, L.; Filippakopoulos, P.; Chung, E.; Yang, Q.; Schwaller, J.; Knapp, S.; King, R. W.; Lee, J.; Herrgard, S.; Zarrinkar, P.; Gray, N. S. *Chem. Biol.* **2011**, *18*, 868.
14. Richardson, C. M.; Nunns, C. L.; Williamson, D. S.; Parratt, M. J.; Dokurno, P.; Howes, R.; Borgognoni, J.; Drysdale, M. J.; Finch, H.; Hubbard, R. E.; Jackson, P. S.; Kierstan, P.; Lentzen, G.; Moore, J. D.; Murray, J. B.; Simmonite, H.; Surgenor, A. E.; Torrance, C. J. *Bioorg. Med. Chem.* **2007**, *17*, 3880.
15. Leeson, P. D.; Springthorpe, B. *Nat. Rev. Drug Disc.* **2007**, *7*, 881.
16. Knoevenagel, E. *Ber.* **1898**, *31*, 2596.
17. (a) Bruno, G.; Constantino, L.; Curinga, C.; Maccari, R.; Monforte, F.; Nicolo, F.; Ottana, R.; Vigorita, M. G. *Bioorg. Med. Chem.* **2002**, *10*, 1077; (b) The Knoevenagel condensation yielded almost exclusively the thermodynamically favored *Z*-isomer (>98:2).; (c) The S_NAr reactions and subsequent Knoevenagel condensations to afford the secondary or primary amine products gave best results when perfomed on the Boc-protected amine starting materials. Boc deprotection under the standard conditions (TFA/DCM or HCl/MeOH) afforded the final amine products as their corresponding salts.
18. The enzyme assays were carried out at [ATP] = K_m for each isozyme. K_m [ATP] values were obtained by fitting the initial velocity of the PIM enzymatic reactions measured by Caliper technology versus ATP substrate concentrations using Michaelis–Menten equation. PIM-1 K_m [ATP] = 100 μM; PIM-2 K_m [ATP] = 5 μM; PIM-3 K_m [ATP] = 50 μM.
19. (a) Tao, Z.; Hasvold, L. A.; Leverson, J. D.; Han, E. K.; Guan, R.; Johnson, E. F.; Stoll, V. S.; Stewart, K. D.; Stamper, G.; Soni, N.; Bouska, J. J.; Luo, Y.; Sowin, T. J.; Lin, N.-H.; Giranda, V. S.; Rosenberg, S. H.; Penning, T. D. *J. Med. Chem.* **2009**, *52*, 6621; (b) Grey, R.; Pierce, A. C.; Bemis, G. W.; Jacobs, M. D.; Moody, C. S.; Jajoo, R.; Mohal, N.; Green, J. *Bioorg. Med. Chem. Lett.* **2009**, *19*, 3019; (c) Qian, K.; Wang, L.; Cywin, C. L.; Farmer, B. T., II; Hickey, E.; Homon, C.; Jakes, S.; Kashem,

M. A.; Lee, G.; Leonard, S.; Li, J.; Magboo, R.; Mao, W.; Pack, E.; Peng, C.; Prokopowicz, A., III; Welzel, M.; Wolak, J.; Morwick, T. *J. Med. Chem.* **1814**, *2009*, 52; (d) Tong, Y.; Stewart, K. D.; Thomas, S.; Przytulinska, M.; Johnson, E. F.; Klinghofer, V.; Leverson, J.; McCall, O.; Soni, N. B.; Luo, Y.; Lin, N.-H.; Sowin, T. J.; Giranda, V. L.; Penning, T. D. *Bioorg. Med. Chem. Lett.* **2008**, *18*, 5206; (e) Pierce, C.; Jacobs, M.; Stuver-Moody, C. *J. Med. Chem.* **2008**, *51*, 1972; (f) Nishiguchi, G. A.; Atallah, G.; Bellamacina, C.; Burger, M. T.; Ding, Y.; Feucht, P. H.; Garcia, P. D.; Han, W.; Klivansky, L.; Lindvall, M. *Bioorg. Med. Chem. Lett.* **2011**, *21*, 6366.

20. Good, A. C.; Liu, J.; Hirth, B.; Asmussen, G.; Xiang, Y.; Biemann, H.-P.; Bishop, K. A.; Fremgen, T.; Fitzgerald, M.; Gladysheva, T.; Jain, A.; Jancsics, K.; Metz, M.; Papoulis, A.; Skerlj, R.; Stepp, J. D.; Wei, R. R. *J. Med. Chem.* **2012**, *55*, 2641.
21. The main chain for the P-loop above the plane of the figure (which contains residue Leu 44 that interacts with the solvent-exposed isopropyl group) has been omitted for the purposes of clarity. Figure produced using Pymol. DeLano, W. L. The PyMOL Molecular Graphics System; DeLano Scientific: San Carlos, CA, USA, 2002. http://www.pymol.org.
22. Matsuo, Y.; Drexler, H. G.; Kaneda, K.; Kojima, K.; Ohtsuki, Y.; Hara, M.; Yasukawa, M.; Tanimoto, M.; Orita, K. *Leuk. Res.* **2003**, *27*, 165.
23. Sanguinetti, M. C.; Tristani-Firouzi, M. *Nature* **2006**, *440*, 463.
24. (a) Karaman, M. W.; Herragard, S.; Treiber, D. K.; Gallant, P.; Atteridge, C. E.; Cambell, B. T.; Chan, K. W.; Ciceri, P.; Davis, M. I.; Edeen, P. T.; Faraoni, R.; Floyd, M.; Hunt, J. P.; Lockhart, D. J.; Milanov, Z. V.; Morrison, M. J.; Pallares, G.; Patel, H. K.; Pritchard, S.; Wodicka, L. M.; Zarrinkar, P. P. *Nat. Biotechnol.* **2008**, *26*, 127; The KinomeScan panel is now division of DiscoveryRx. http://www.kinomescan.com/.
25. Image generated using TREEspot™ Software Tool and reprinted with permission from KINOMEscan™, a division of DiscoveRx Corporation, ©DISCOVERX CORPORATION 2010.